Analytical and Bioanalytical Chemistry
https://doi.org/10.1007/s00216-021-03603-1

RESEARCH PAPER

Electrochemical impedance biosensor for detection of saxitoxin in aqueous solution

Pablo C. Serrano[1] · Gisele E. Nunes[1] · Lindiomar B. Avila Jr[1] · Carleane P.S. Reis[1] · Aldo M.C. Gomes[1] · Françoise T. Reis[1] · Maria L. Sartorelli[1] · Silvia Pedroso Melegari[2] · William G. Matias[3] · Ivan H. Bechtold[1]

Received: 14 May 2021 / Revised: 26 July 2021 / Accepted: 5 August 2021
© Springer-Verlag GmbH Germany, part of Springer Nature 2021

Abstract

Saxitoxin is a cyanotoxin which is very harmful to human health; the concentration limit in drinking water is only 3 μg/L. Therefore, a simple, fast, sensitive, low-cost, and specific method for its detection, quantification, and monitoring in water bodies is needed to avoid adverse effects on animal and human health. In this work, we developed an electrochemical impedimetric biosensor using a specific aptamer as recognition element for saxitoxin detection. This method allies the superior sensing characteristics of aptamers with the nondestructive, label-free, and easy working principles of the electrochemical impedance technique. The device presented sensitivity for detecting saxitoxin concentrations above 0.3 μg/L, with high selectivity in negative control experiments, demonstrating a promising alternative for water toxin detection.

Keywords Biosensor · Saxitoxin · Electrochemical impedance spectroscopy · Aptamer

Introduction

The pollution of rivers, reservoirs, and lakes have affected the water resources quality in recent decades. Consequently, cyanobacterial blooms can occur, causing economic, environmental, and public health problems related to water supply [1]. Algal blooms cause negative impacts for water bodies worldwide, often producing undesirable color, odor, and taste. Under certain conditions, species in harmful algal blooms (HABs) can produce toxins that can harm human health, animals, and the aquatic ecosystems [1–3]. Human poisoning outbreaks associated to toxic cyanobacteria have been reported around the world: in Brazil, a well-known severe human poisoning episode occurred in the city of Caruaru (northeastern Brazil) in 1996, in a hemodialysis clinic, leading over 50 patients to death [1, 4]. In the Peri Lagoon, a shallow lake in the city of Florianopolis (southern Brazil), some toxic algal blooms have already been found. The presence of saxitoxin (STX) was recorded in Peri Lagoon water and can be attributed to *Cylindrospermopsis raciborskii* cyanobacterial species, which is a toxic phytoplankton [5, 6].

STX is a potent neurotoxin with low molecular weight (299 g/mol) and molecular structure $C_{10}H_7N_7O_4$, belonging to the paralytic shellfish poisoning (PSP) toxin group [7, 8]. Since STX can enter the food chain by accumulating in filter-feeding bivalves and fishes, there is a preeminent risk to human health [9, 10]. The exposure to this toxin can induce numbness, headache, tingling, muscle weakness, respiratory failure and even death [10]. The guidance concentration limit for STX in drinking water, in most countries is 1–3 μg/L [7]. The value recommended by the Brazilian Health Ministry's legislation is 3 μg/L [6].

The main methods and analyses for the detection of water toxins can be listed into four broad groups [11]: mouse bioassay (MBA) [12], enzyme-linked immunosorbent assay (ELISA) [13], high-performance liquid chromatography (HPLC) [14], and liquid chromatography-mass spectrometry (LC-MS) [15]. The MBA has been the longstanding regulated official method for STX analysis [8, 16]. It offers adequate measurements, however, presenting disadvantages, including poor specificity and low sensitivity, in addition to ethical issues related to the use of live animals [8, 10, 17]. Analytical

✉ Ivan H. Bechtold
ivan.bechtold@ufsc.br

[1] Departamento de Física, Universidade Federal de Santa Catarina, Florianópolis, SC 88040-900, Brazil

[2] Centro de Estudos do Mar, Universidade Federal do Paraná, Pontal do Paraná, PR 83255-976, Brazil

[3] Departamento de Engenharia Sanitária e Ambiental, Universidade Federal de Santa Catarina, Florianópolis, SC 88040-900, Brazil

Published online: 13 August 2021

methods, such as HPLC and its coupled techniques, allow for the selective identification, separation, and sensitive quantification; on the other hand, it requires highly skilled and trained personnel, toxin reference standards, expensive and sophisticated equipment, and time-consuming procedures [9, 10]. Immunoassay has been suitably used as routine detection and quantification, since it does not require expensive instrumentation and trained people to operate, nevertheless, it is rather expensive [13]. More recently, colorimetric assay [18, 19] and photoelectrochemical immunoassay [20–22] methods have been successfully applied for toxin detection.

Biosensors might offer a simple, sensitive, effective, and suitable alternative technique for monitoring, quantification, and toxin detection [11, 23]. Electrochemical impedance spectroscopy (EIS) is a sensitive and excellent method for monitoring the interaction between biorecognition elements immobilized onto the electrode surface, and target analytes, which can be used to determine quantitative responses of electrochemical parameters [2, 23]. Using EIS, one can evaluate changes in the capacitance and in the charge transfer resistance(R_{ct}) at the interface between electrode surface and the electrolyte, when target molecules (i.e., toxins) are captured by biorecognition elements, such as antibodies and aptamers [24–26].

Aptamers (APTs) consist of nucleic acid oligomers (RNA or DNA molecules), which can bind to a wide range of specific target analytes, with high affinity and selectivity [27]. While antibody production requires in vivo conditions, APTs can be chemically synthesized in vitro [28]. Due to this and other advantages, such as high stability and especially the fact that they can be easily modified via chemical reactions to introduce functional groups, APTs are a promising choice for biosensing [27, 29]. Some APTs targeting toxins have been selected in the last 10 years, such as ochratoxin A [30], okadaic acid [31], microcystin-LR (MCLR) [32], and even STX [16, 17]. In 2013, a DNA aptamer (APT^{STX1}) for STX was reported for the first time by Handy et al. [17]. In 2015, Zheng et al. [16] obtained an APT with 30-fold (M-30f) higher binding for STX, compared with APT^{STX1}. Some biosensors using APT as biorecognition element for STX have been developed, based on amperometric [8], potentiometric [7], fluorescence [10, 33], and colorimetric analyses [34] and surface-enhanced Raman scattering detection [35, 36].

The advantages of the electrochemical impedimetric aptasensor can be understood in terms of the superior sensing characteristics of aptamers, such as high specificity of binding affinity, better stabilization, and longer shelf life when compared to antibodies [23, 37]. In addition, unlike voltammetric techniques, electrochemical impedance is nondestructive to the biological interactions, since it works under very small amplitude perturbation from steady state, and it is also considered a label-free technique, as it does not require special tagging or reagents [23, 38]. Label-free impedimetric aptasensors have been an effective alternative for the detection and quantification of several toxins, such as microcystin-LR (MCLR) [39], okadaic acid [31], anatoxin-a [40], and cylindrospermopsin [41]. In this work, the APT (M-30f) [16] was functionalized with thiol for immobilization onto the gold electrode surface to act as biorecognition element for electrochemical detection of STX. Combining the high affinity and selectivity of APT (M-30f) with the high sensitivity of EIS, we developed a novel, simple, and stable label-free impedimetric aptasensor for STX rapid detection in aqueous solution.

Experimental

Materials and reagents

The oligonucleotide sequence of the APT (M-30f) [16] was functionalized with a thiol group at its 3′-end, to allow immobilization on the gold electrode surface. The sequence was purchased from INNOVARE Diagnóstico (Brazil), as follows:

(5′-T TGA GGG TCG CAT CCC GTG GAA ACA GGT TCA TTG AAA AAA AAA AA-C_6S-S-3′).

STX and MCLR were obtained from the National Research Council of Canada. Phosphate-buffered saline (PBS), Tris-HCl, EDTA disodium dihydrate, ethanol, boric acid, potassium ferrocyanide ($K_4Fe(CN)_6$), potassium ferricyanide ($K_3Fe(CN)_6$), sodium chloride (NaCl), 6-mercapto-1-hexanol (MCH), magnesium chloride ($MgCl_2$), KOH, and H_2O_2 were purchased from Sigma-Aldrich (Brazil). The following buffers were used in the electrochemical experiments: Tris-EDTA buffer (TE buffer) consists of 10 mM Tris, pH 7.4, and 1 mM EDTA; phosphate buffer solution (10 mM, pH 7.4); binding buffer consists of 50 mM Tris-HCl, pH 7.5, 150 mM NaCl, and 2 mM $MgCl_2$.

Preparation of the biosensor

Initially, the gold (Au) electrodes (3 mm in diameter, 5 nm chrome/50 nm Au) were polished with 0.5 μm alumina (Al_2O_3) particles; then, the electrodes were ultrasonically cleaned in ultrapure water and dried with nitrogen stream. The electrodes were placed in 50 mM KOH and 25% H_2O_2 solution during 10 min and washed with ultrapure water. Finally, electrochemical sweep in 50 mM KOH solution by cyclic voltammetry (CV) scanning from 200 to 1200 mV (vs. Ag/AgCl) at 50-mV/s scan rate was performed and then rinsed in ultrapure water. The solution containing 1 μM thiolated APT was immobilized by drop-casting on the Au electrode a 5-μL droplet, at 37 °C, for 1 h. The Au/APT electrode was

rinsed with the TE buffer solution to remove excess. This system was incubated in 1 mM of MCH in phosphate buffer, for 1 h, to cover the nonactive sites of the Au/APT surface. The modified Au/APT/MCH electrode was incubated in the STX concentrations of interest in the binding buffer, during 1 h, at 4 °C. The final structure Au/APT/MCH/STX was then washed with the binding buffer, to remove the nonspecifically bounded STXs. The electrochemical measurements were performed after each step of the electrode preparation.

Electrochemical measurements

The CV and EIS experiments were performed with an AutoLab PGSTAT302N potentiostat/galvanostat/frequency-response analyzer, controlled by NOVA 2.1 software. A three-electrode electrochemical cell was used: the gold electrode as the working electrode; Ag/AgCl saturated with KCl as reference electrode; and a platinum plate as counter electrode. For the CV experiments, a scan rate of 50 mV/s was used. The EIS measurements were recorded with 10 mV amplitude sinusoidal signal, at the open circuit potential (OCP) (0.22 V/Ag/AgCl), in the frequency range between 100 kHz to 100 mHz. All measurements were performed in 10 mM PBS buffer, pH 7.4, and in the presence of 5 mM $[Fe(CN)_6]^{3-}$/$Fe[(CN)_6]^{4-}$ redox-pair solution.

Results and discussion

The aptasensor performance to detect STX certainly depends on the STX incubation time. Figure 1 a shows the responses of the aptasensor at different incubation times for 30 μg/L STX solution. The impedimetric aptasensor response $\Delta R_{ct} = 1 - R/R_0$, which represents the percentage change in the impedance R_{ct} before (R_0) and after (R) binding, was used to evaluate the STX detection. The impedimetric aptasensor response increased rapidly in the first 30 min, reaching 55%. After 1 h, around 80% is obtained, followed by a slight increase of 10% from 1 to 5 h, which illustrates saturation of the label-free impedimetric aptasensor. Thus, 1 h was used as the optimum STX binding time in further experiments. Other reported aptasensors for toxins used closely the same incubation time [8, 31, 40]. No difference on the impedance curves was observed for APT drying times longer than 1 h. The incubation of the modified APT electrode in MCH for more than 1 h did not improve device performance, which agrees with the fact that MCH quickly saturates onto the gold electrode [31, 40, 41].

Figure 1 b shows the CV measurements for each construction step of the biosensor, where the $[Fe(CN)_6]^{3/4-}$ redox couple exhibited a characteristic quasi-reversible voltammogram on the bare Au electrode, with a 90-mV peak-to-peak separation. After the APT immobilization, the electrochemical reaction is inhibited, verified by the increase in the peak separation

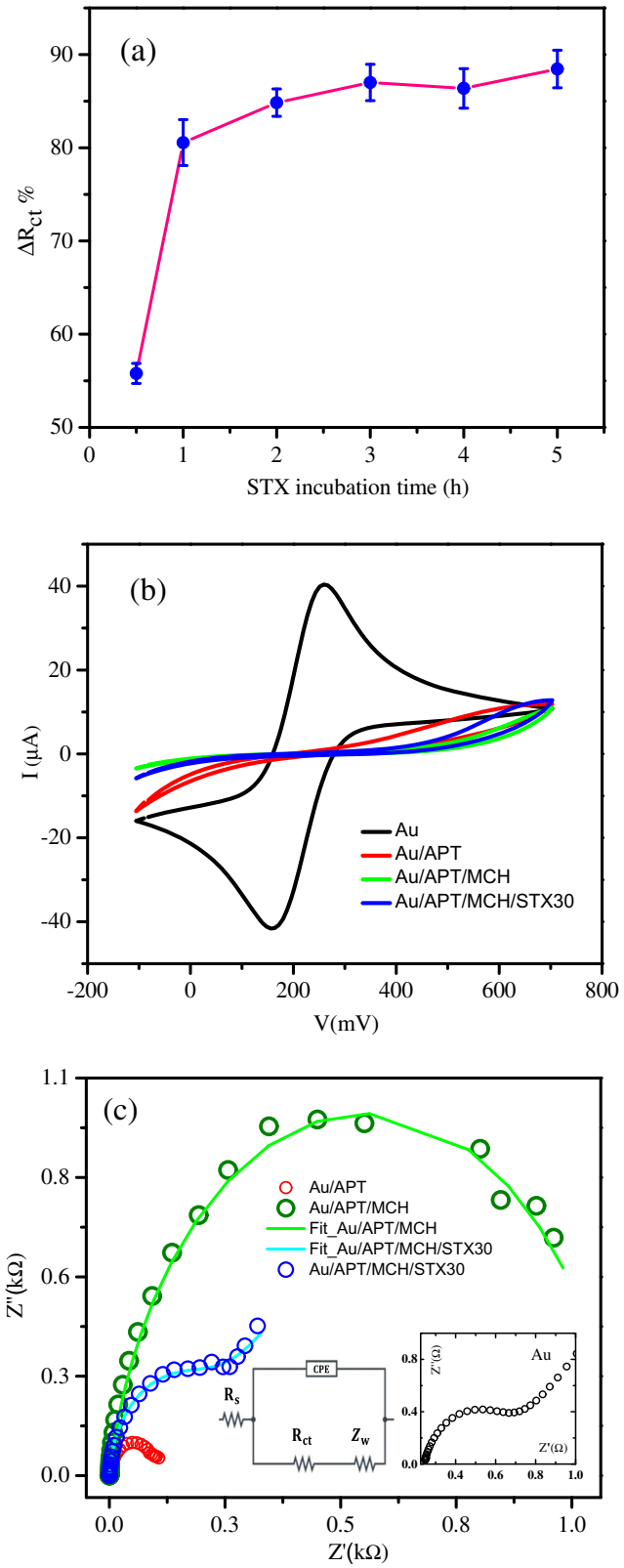

Fig. 1 **a** STX incubation time. **b** Cyclic voltammograms and **c** Nyquist diagram normalized for the aptasensor by drop-casting deposition in 5 mM solution of $[Fe(CN)_6]^{3-/4-}$ in PBS, pH = 7.4. Inset, the equivalent circuit used for fitting the experimental curves (solid lines)

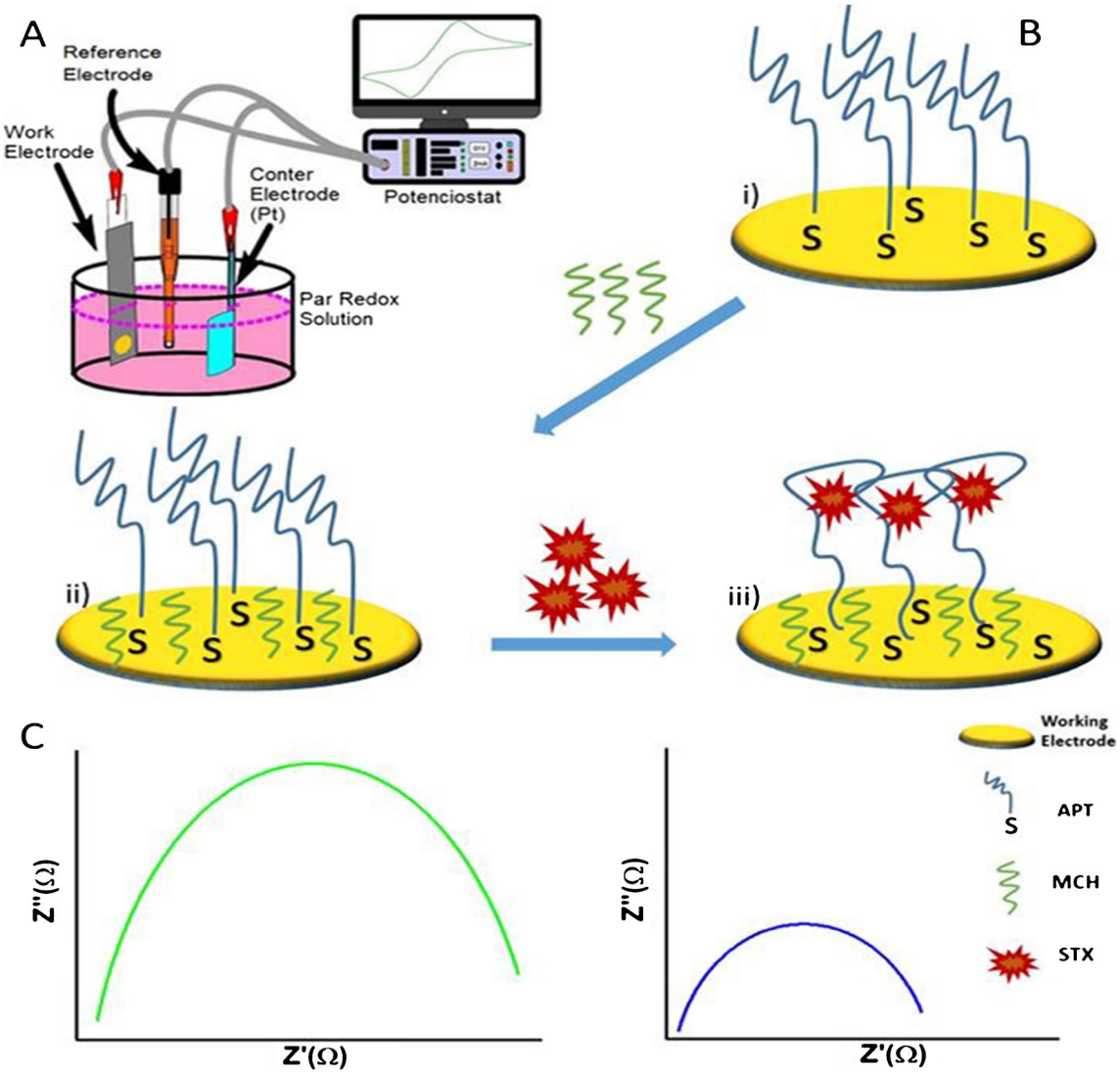

Fig. 2 **A** Electrochemical system. **B** Principle of aptasensor operation. Device modification steps based on an APT for STX detection and **C** impedance curves of the biosensor steps

and the decrease in the peak current. This change might result from electrostatic repulsion between the immobilized APT and $[Fe(CN)_6]^{3-/4-}$ anions, both negatively charged, making the access of the redox couple to the Au electrode surface difficult [31, 40, 41]. A further increase in the peak-to-peak separation was observed after filling the free space of the electrode with MCH, indicating an additional decrease of the electron-transfer rate. Finally, after the STX incubation, an increase in the intensity of the current peak is observed. Therefore, lowering the exposed negative charge may facilitate the electronic exchange between the redox pair and the gold electrode surface [31, 40, 41].

Figure 1 c shows the Nyquist diagram for each electrode modification step. This impedance representation of an electrochemical biosensor usually consists of a semicircular part at higher frequencies, corresponding to an electron-transfer process, and often presents a linear low-frequency region, which represents the diffusion limited process [42, 43]. The diameter of the semicircle corresponds to charge transfer resistance(R_{ct}). The ferric/ferrous cyanide ion pair $[Fe(CN)_6]^{3-/4-}$ is the redox probe often used for electrochemical measurement in an impedimetric biosensor of algal toxins in water [2]. In the inset of Fig. 1c, the bare Au electrode curve shows a fast electron-transfer step, followed by a diffusion limited process at low frequencies. After APT immobilization onto the Au electrode, the semicircle diameter increases, which might be attributed to a higher R_{ct} due to repulsion of the APT on the electrode surface with $[Fe(CN)_6]^{3-/4-}$ anions in the solution [31, 40, 41]. As expected, the incubation with MCH resulted in further increase of the R_{ct}, due to the covering of the exposed gold areas by MCH, which introduces a barrier to the interfacial electron transfer. After the STX binding to APT, a decrease in the R_{ct} occurs, suggesting conformation changes of APT and/or electrostatic repulsion between

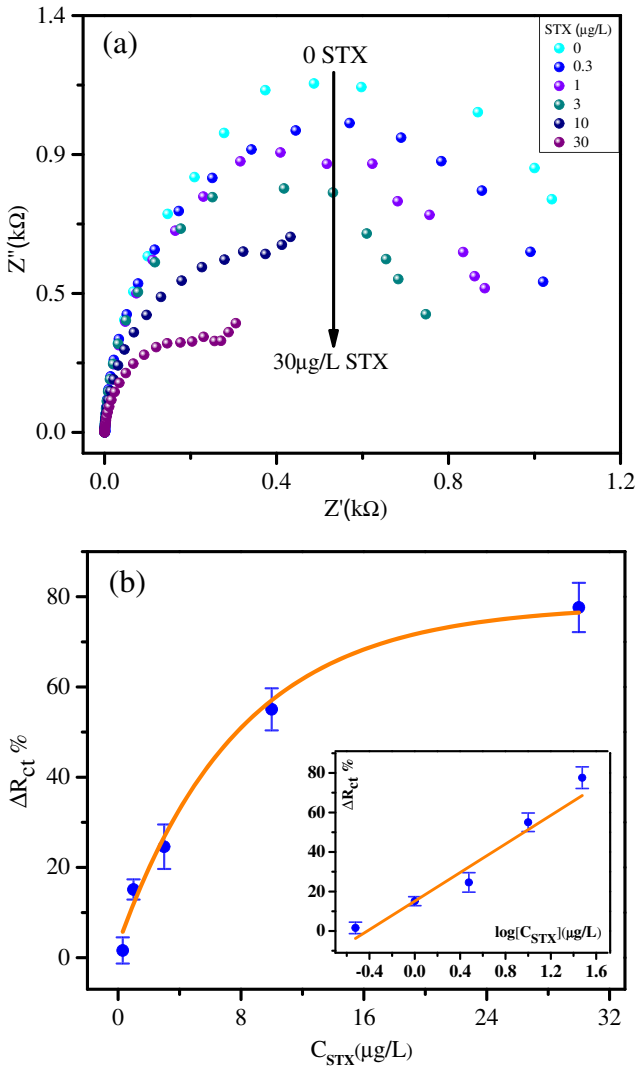

Fig. 3 **a** Nyquist diagram normalized for the impedimetric aptasensor after incubation at different concentrations, 0.3, 1; 3; 10; and 30 µg/L of STX. **b** The calibration curve for STX, plot of impedance increase rate $\Delta R_{ct} = 1 - R/R_0$ vs STX concentration (C_{STX}), inset linear relationship between ΔR_{ct} vs a function of the log STX concentration log[C_{STX}]

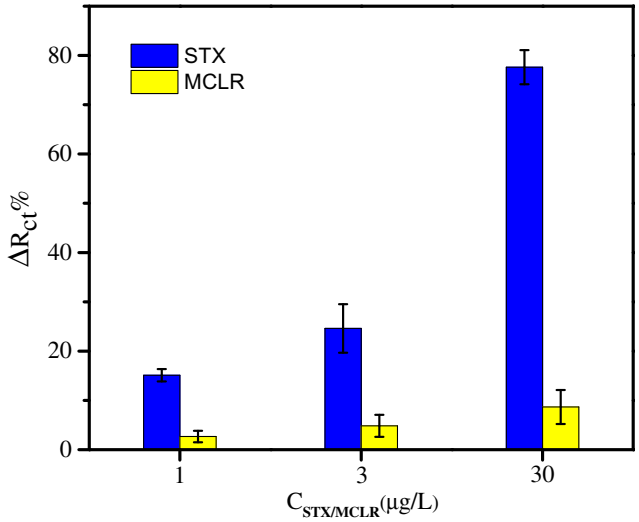

Fig. 4 Negative control: comparison of label-free impedimetric aptasensor response after incubation with STX and MCLR for different toxin concentrations

the free charges of the target molecules (STX) and the electroactive species in the supporting electrolyte [23], indicating the formation of the APT-STX complex. This result is in accordance with the CV behavior and agrees with studies published in the literature, concerning other toxins produced by toxic algae [31, 39–41]. The impedance spectra were fitted with a modified Randles equivalent circuit (inset of Fig. 1b), consisting of the solution resistance (R_s), a constant phase element (CPE), a charge transfer resistance (R_{ct}), and a Warburg impedance(Z_w) [42, 43].

Figure 2 illustrates the working principle and the construction steps of the device. The APT adhesion on the Au electrode (Fig. 2B) occurs due to the well-known strong Au-S chemical bond of the thiol group functionalized at the 3′-end of the APT. The Au/APT electrode blocking with MCH is of fundamental importance, to assure that the response of the next detection step arises only from the specific interaction between STX and APT. The STX-APT binding causes a change in the impedimetric signal, registered by the decrease of R_{ct} (Fig. 2C). Many impedimetric biosensors for toxin detection, using APTs as biorecognition element, show such behavior after the APT-toxin interaction [31, 39–41], attributed to conformation changes of the APT and/or electrostatic repulsion between the free charges of the target molecules and the electroactive species in the supporting electrolyte [23].

The impedimetric biosensor response to different concentrations of STX in the range between 0.3 and 30 µg/L is presented in Fig. 3a. After incubation with STX, a decrement in R_{ct} was observed by increasing the STX concentration, which may be due to conformation change of the immobilized APTs upon STX recognition and/or electrostatic repulsion between the free charges of STX and the electroactive species in the supporting electrolyte [23], as indicated before. The immobilization of APT by drop-casting onto the gold electrode produced nonuniform and thick films, which may interfere in the charge transfer across the electrode/electrolyte interface producing an electrochemical system kinetically sluggish with a significantly large R_{ct} [43] and some slightly scattered points on the impedance spectra [42]. Nevertheless, the results in this work are quite reproducible.

The impedance decrease rate $\Delta R_{ct} = 1 - R/R_0$ for the modified gold electrode (Au/APT/MCH), before (R_0) and after (R) STX binding, was calculated. Figure 3b shows the calibration curve after incubation for different STX concentrations. The points in the calibration curve of Fig. 3b represent the average of two independent measurements. Inset, a linear regression equation $\Delta R_{ct} = 0.175 + 0.378 \log[C_{STX}]$, with a correlation coefficient of 0.994, obtained when the STX concentration is set on a

logarithmic scale. A limit of detection (LOD) of 0.3 μg/L was estimated from the equation $3S/m$ [31, 39–41], where S is the standard deviation of the impedance measurement and m is the slope of the calibration curve (inset of Fig. 3b).

The specificity of the proposed label-free impedimetric aptasensor was analyzed through negative control experiments, by incubating the APT-modified Au electrode in a microcystin-LR (MCLR) solution, Au/APT/MCH, which is also a toxin produced by cyanobacteria, but not specific to the APT recognition element used in the present work. Figure 4 shows ΔR_{ct} corresponding to 1, 3, and 30 μg/L for both toxins, indicating that there is not a significant change in the R_{ct} in the presence of MCLR compared to the case of STX, evidencing the high selectivity of the device.

Conclusion

We have successfully developed a label-free impedimetric aptasensor for fast saxitoxin detection, using an aptamer as specific biorecognition element with high affinity and remarkable sensitivity and stability. The obtained limit of detection was 0.3 μg/L, which corresponds to 10% of the limit concentration of STX allowed in drinking water (3 μg/L). Moreover, it presented high selectivity in negative control experiments, including a different cyanobacteria toxin, demonstrating to be a promising alternative for water toxin detection. The method allowed for the monitoring of the electrochemical parameters in each step of the electrode modification, in order to discuss the working principle of the device. Finally, for future application prospective, the biosensor will be tested on real water samples from the Peri Lagoon, using the calibration curve performed in aqueous solution.

Funding This work received financial support from the Conselho Nacional de Desenvolvimento Científico e Tecnológico (CNPq), Coordenação de Aperfeiçoamento de Pessoal de Nível Superior (CAPES), Fundação de Amparo à Pesquisa e Inovação do Estado de Santa Catarina (FAPESC), and Instituto Nacional de Ciência e Tecnologia em Eletrônica Orgânica (INCT/INEO).

Declarations

Conflict of interest The authors declare no competing interests.

References

1. Chorus I, Welker M, editors. Toxic cyanobacteria in water. 2nd ed. Oxfordshire: Taylor & Francis; 2021.
2. Zhang W, Dixon MB, Saint C, Teng KS, Furumai H. Electrochemical biosensing of algal toxins in water: the current state-of-the-art. ACS Sens. 2018;3(7):1233–45. https://doi.org/10.1021/acssensors.8b00359.
3. Munoz M, Nieto-Sandoval J, Cirés S, de Pedro ZM, Quesada A, Casas JA. Degradation of widespread cyanotoxins with high impact in drinking water (microcystins, cylindrospermopsin, anatoxin-a and saxitoxin) by CWPO. Water Res. 2019;163(10):114853. https://doi.org/10.1016/j.watres.2019.114853.
4. Azevedo SMFO, et al. Human intoxication by microcystins during renal dialysis treatment in Caruaru-Brazil. Toxicology. 2002;181–182(12):441–6. https://doi.org/10.1016/S0300-483X(02)00491-2.
5. Baptista M, Nixdorf B. Low disturbances favor steady state: case of cyanobacterial monodominance in a Brazilian coastal lagoon. Inl Waters. 2014;4(2):243–54. https://doi.org/10.5268/IW-4.2.648.
6. Ramos TK, et al. Saxitoxins from the freshwater cyanobacterium Raphidiopsis raciborskii can contaminate marine mussels. Harmful Algae. 2021;103(3):102004. https://doi.org/10.1016/j.hal.2021.102004.
7. Bratakou S, Nikoleli G-P, Siontorou CG, Nikolelis DP, Karapetis S, Tzamtzis N. Development of an electrochemical biosensor for the rapid detection of saxitoxin based on air stable lipid films with incorporated anti-STX using graphene electrodes. Electroanalysis. 2017;29(4):990–7. https://doi.org/10.1002/elan.201600652.
8. Hou L, et al. Amperometric aptasensor for saxitoxin using a gold electrode modified with carbon nanotubes on a self-assembled monolayer, and methylene blue as an electrochemical indicator probe. Microchim Acta. 2016;183(6):1971–80. https://doi.org/10.1007/s00604-016-1836-1.
9. Gao S, Zheng X, Wu J. A biolayer interferometry-based competitive biosensor for rapid and sensitive detection of saxitoxin. Sensors Actuators B Chem. 2017;246(7):169–74. https://doi.org/10.1016/j.snb.2017.02.078.
10. Cheng S, et al. Study of the binding way between saxitoxin and its aptamer and a fluorescent aptasensor for detection of saxitoxin. Spectrochim Acta Part A Mol Biomol Spectrosc. 2018;204:180–7. https://doi.org/10.1016/J.SAA.2018.06.036.
11. Ye W, et al. Marine toxins detection by biosensors based on aptamers. Toxins. 2019;12(1):1. https://doi.org/10.3390/toxins12010001.
12. Cheng J, et al. A new simple screening method for the detection of paralytic shellfish poisoning toxins. Chin J Oceanol Limnol. 2012;30(5):786–90. https://doi.org/10.1007/s00343-012-1097-8.
13. Ling S, et al. Preparation of monoclonal antibody for brevetoxin 1 and development of Ic-ELISA and colloidal gold strip to detect brevetoxin 1. Toxins (Basel). 10(2):75. https://doi.org/10.3390/toxins10020075.
14. Halme M, Rapinoja ML, Karjalainen M, Vanninen P. Verification and quantification of saxitoxin from algal samples using fast and validated hydrophilic interaction liquid chromatography-tandem mass spectrometry method. J Chromatogr B Anal Technol Biomed Life Sci. 2012;880(1):50–7. https://doi.org/10.1016/j.jchromb.2011.11.015.
15. Krock B, et al. LC-MS/MS detection of karlotoxins reveals new variants in strains of the marine dinoflagellate karlodinium veneficum from the ebro delta (NW mediterranean). Mar Drugs. 2017;15(12):391. https://doi.org/10.3390/md15120391.
16. Zheng X, et al. A saxitoxin-binding aptamer with higher affinity and inhibitory activity optimized by rational site-directed mutagenesis and truncation. Toxicon. 2015;101:41–7. https://doi.org/10.1016/j.toxicon.2015.04.017.
17. Handy SM, et al. First report of the use of a saxitoxin-protein conjugate to develop a DNA aptamer to a small molecule toxin. Toxicon. 2013;61(1):30–7. https://doi.org/10.1016/j.toxicon.2012.10.015.
18. Lai W, Wei Q, Zhuang J, Lu M, Tang D. Fenton reaction-based colorimetric immunoassay for sensitive detection of brevetoxin B. Biosens Bioelectron. 2016;80:249–56. https://doi.org/10.1016/j.bios.2016.01.088.

19. Lai W, Zhuang J, Tang D. Novel colorimetric immunoassay for ultrasensitive monitoring of brevetoxin b based on enzyme-controlled chemical conversion of sulfite to sulfate. J Agric Food Chem. 2015;63(7):1982–9. https://doi.org/10.1021/acs.jafc.5b00425.
20. Lin Y, Zhou Q, Tang D. Dopamine-loaded liposomes for in-situ amplified photoelectrochemical immunoassay of AFB1 to enhance photocurrent of Mn2+-doped Zn3(OH)2V2O7 nanobelts. Anal Chem. 2017;89(21):11803–10. https://doi.org/10.1021/acs.analchem.7b03451.
21. Lin Y, Zhou Q, Tang D, Niessner R, Knopp D. Signal-on photoelectrochemical immunoassay for aflatoxin B1 based on enzymatic product-etching MnO2 nanosheets for dissociation of carbon dots. Anal Chem. 2017;89(10):5637–45. https://doi.org/10.1021/acs.analchem.7b00942.
22. Lin Y, Zhou Q, Zeng Y, Tang D. Liposome-coated mesoporous silica nanoparticles loaded with L-cysteine for photoelectrochemical immunoassay of aflatoxin B1. Microchim Acta. 2018;185(6):1–9. https://doi.org/10.1007/s00604-018-2848-9.
23. Bahadır EB, Sezgintürk MK. A review on impedimetric biosensors. Artif Cells Nanomed Biotechnol. 2016;44(1):248–62. https://doi.org/10.3109/21691401.2014.942456.
24. Xu M, Gao Z, Wei Q, Chen G, Tang D. Hemin/G-quadruplex-based DNAzyme concatamers for in situ amplified impedimetric sensing of copper(II) ion coupling with DNAzyme-catalyzed precipitation strategy. Biosens Bioelectron. 2015;74:1–7. https://doi.org/10.1016/j.bios.2015.05.056.
25. Qiu Z, Tang D, Shu J, Chen G, Tang D. Enzyme-triggered formation of enzyme-tyramine concatamers on nanogold-functionalized dendrimer for impedimetric detection of Hg(II) with sensitivity enhancement. Biosens Bioelectron. 2016;75:108–15. https://doi.org/10.1016/j.bios.2015.08.026.
26. Hou L, Wu X, Chen G, Yang H, Lu M, Tang D. HCR-stimulated formation of DNAzyme concatamers on gold nanoparticle for ultrasensitive impedimetric immunoassay. Biosens Bioelectron. 2015;68:487–93. https://doi.org/10.1016/j.bios.2015.01.043.
27. Kong HY, Byun J. Nucleic acid aptamers: new methods for selection, stabilization, and application in biomedical science. Biomolecul Therapeut. 2013;21(6):423–34. https://doi.org/10.4062/biomolther.2013.085.
28. Bazin I, Tria SA, Hayat A, Marty J-L. New biorecognition molecules in biosensors for the detection of toxins. Biosens Bioelectron. 2017;87:285–98. https://doi.org/10.1016/j.bios.2016.06.083.
29. Zhou W, Jimmy Huang P-J, Ding J, Liu J. Aptamer-based biosensors for biomedical diagnostics. Analyst. 2014;139(11):2627. https://doi.org/10.1039/c4an00132j.
30. Cruz-Aguado JA, Penner G. Determination of ochratoxin A with a DNA Aptamer. J Agric Food Chem. 2008;56(22):10456–61. https://doi.org/10.1021/jf801957h.
31. Eissa S, Ng A, Siaj M, Tavares AC, Zourob M. Selection and identification of DNA aptamers against okadaic acid for biosensing application. Anal Chem. 2013;85(24):11794–801. https://doi.org/10.1021/ac402220k.
32. Ng A, Chinnappan R, Eissa S, Liu H, Tlili C, Zourob M. Selection, characterization, and biosensing application of high affinity congener-specific microcystin-targeting aptamers. Environ Sci Technol. 2012;46(19):10697–703. https://doi.org/10.1021/es301686k.
33. Alfaro K, Bustos P, O'Sullivan C, Conejeros P. Facile and cost-effective detection of saxitoxin exploiting aptamer structural switching. Food Technol Biotechnol. 2015;53(3):337–41. https://doi.org/10.17113/ftb.53.03.15.3911.
34. Zhong L, et al. Portable smartphone-based colorimetric analyzer with enhanced gold nanoparticles for on-site tests of seafood safety. Anal Sci. 2019;35(2):133–40. https://doi.org/10.2116/analsci.18P184.
35. Cheng S, et al. Determination of saxitoxin by aptamer-based surface-enhanced raman scattering. Anal Lett. 2019;52(6):902–18 https://doi.org/10.1080/00032719.2018.1505900.
36. Caglayan MO, Üstündağ Z. Saxitoxin aptasensor based on attenuated internal reflection ellipsometry for seafood. Toxicon. 2020;187:255–61. https://doi.org/10.1016/j.toxicon.2020.09.005.
37. Erdem A, Congur G. Dendrimer modified 8-channel screen-printed electrochemical array system for impedimetric detection of activated protein C. Sensors Actuators B Chem. 2014;196:168–74. https://doi.org/10.1016/j.snb.2014.01.103.
38. Elshafey R, Tavares AC, Siaj M, Zourob M. Electrochemical impedance immunosensor based on gold nanoparticles–protein G for the detection of cancer marker epidermal growth factor receptor in human plasma and brain tissue. Biosens Bioelectron. 2013;50:143–9. https://doi.org/10.1016/j.bios.2013.05.063.
39. Lin Z, et al. Determination of microcystin-LR in water by a label-free aptamer based electrochemical impedance biosensor. Talanta. 2013;103:371–4. https://doi.org/10.1016/j.talanta.2012.10.081.
40. Elshafey R, Siaj M, Zourob M. DNA aptamers selection and characterization for development of label-free impedimetric aptasensor for neurotoxin anatoxin-a. Biosens Bioelectron. 2015;68:295–302. https://doi.org/10.1016/j.bios.2015.01.002.
41. Elshafey R, Siaj M, Zourob M. In vitro selection, characterization, and biosensing application of high-affinity cylindrospermopsin-targeting aptamers. Anal Chem. 2014;86(18):9196–203. https://doi.org/10.1021/ac502157g.
42. Lasia A. Electrochemical impedance spectroscopy and its applications. 1st ed. New York: Springer; 2014.
43. Yuan X-Z, Song C, Wang H, Zhang J. Electrochemical impedance spectroscopy in PEM fuel cells. London: Springer London; 2010.

Publisher's note Springer Nature remains neutral with regard to jurisdictional claims in published maps and institutional affiliations.